Numerical simulation of a thermoacoustic couple

Ahmed Abd El-Rahman, Ehab Abdel-Rahman

▶ **To cite this version:**

Ahmed Abd El-Rahman, Ehab Abdel-Rahman. Numerical simulation of a thermoacoustic couple. Acoustics 2012, Apr 2012, Nantes, France. hal-00810707

HAL Id: hal-00810707
https://hal.science/hal-00810707

Submitted on 23 Apr 2012

HAL is a multi-disciplinary open access archive for the deposit and dissemination of scientific research documents, whether they are published or not. The documents may come from teaching and research institutions in France or abroad, or from public or private research centers.

L'archive ouverte pluridisciplinaire **HAL**, est destinée au dépôt et à la diffusion de documents scientifiques de niveau recherche, publiés ou non, émanant des établissements d'enseignement et de recherche français ou étrangers, des laboratoires publics ou privés.

Numerical simulation of a thermoacoustic couple

A. I. Abd El-Rahman[a] and E. Abdel-Rahman[b,c]

[a]Department of Physics, American University in Cairo, AUC Avenue, P.O. Box 74, 11835 New Cairo, Egypt
[b]American University in Cairo, Department of Physics - School of Sciences & Engineering, Youssef Jameel Science and Technology Research Centre (YJSTRC), 11835 New Cairo, Egypt
[c]Mechanical Power Engineering Department, Cairo University, 12613 Cairo, Egypt
ahmedibrahim@aucegypt.edu

Here we report a two-dimensional computational fluid dynamics (CFD) simulation of the non-linear oscillating-flow behavior in a helium-filled half-wavelength thermoacoustic refrigerator. The finite volume method is used, and the solid and air domains are represented by large numbers of quadrilateral and triangular elements. The calculations assume a periodic structure to reduce the computational cost and apply the dynamic mesh technique to account for the oscillating adiabatic equivalent wall boundaries. The simulation uses an implicit time integration of the full unsteady compressible flow equations with a conjugate heat transfer algorithm (ANSYS FLUENT). A Typical run involves 12000 elements and a total simulation time of five seconds. Simulation Results for drive ratios range $0.28\% - 2\%$ are compared to the Swift linear theory and the numerical analysis of Worlikar *et al*, and show better agreement with the experimental values of Atchley. A maximum cooling effect of three degrees is predicted at a non-dimensional wave number $3\pi/4$, measured from the resonator rigid end. This simulation provides an interesting tool for understanding the bulk and micro-structural flow behavior and the associated nonlinear acoustic streaming in thermoacoustic refrigerators, characterizing and optimizing their performance, and building models of thermoacoustic flow analysis.

1 Introduction

A thermoacoustic refrigerator (TAR) is a device that is mainly consisting of a resonator, a stack and two heat exchangers. Typically, the resonator is a long circular tube filled with working gas, while the stack has small and relatively low thermal conductivity and high specific heat ceramic parallel plates aligned with the direction of the prevailing resonant wave. The resonator of a standing-wave refrigerator has one end closed and is bounded by the acoustic driver at the other end enabling the propagation of half-wavelength acoustic excitation. The hot and cold heat exchangers are made of copper to allow for efficient heat transfer between the working gas and the external heat source and sink respectively.

TARs are attractive because they have no moving parts, unlike conventional refrigerators, and almost no environmental impact exists as they rely on the conversion of acoustic and heat energies. Their fabrication process is rather simpler and sizes span wide variety of length scales. The viscous and thermal interactions between the stack plates, heat exchangers' plates and the working gas significantly affect the flow field within the plates' channels, as explained by Panton [5], and the energy flux density at the plates' surfaces, respectively. In typical low-pressure excitation systems, the thermoacoustic behavior is dominated by the Swift [1] linear theory. However, practical TARs fall into the high-pressure-amplitude regime of wave propagation, where non-linear behavior is frequent, and so the need to introduce a computational fluid dynamics analysis that solves the fully coupled non-linear compressible flow equations has considerable importance.

This work numerically simulates the non-linear oscillating flow behavior exhibited in half-wavelength thermoacoustic refrigerators and predicts the thermoacoustic cooling effect between the stack ends and calculates the amount of the converted acoustic power. The current numerical results are compared to the experimental measurements of Atchley [4]. The analysis below uses the ANSYS FLUENT second-order finite-volume implicit-time-algorithm CFD solver with the k-ε turbulence model and the conjugate heat transfer algorithm. This work predicts the general behavior of TARs and examines the evolved microstructural vortices and the acoustic flow streaming and presents a stepping stone in building a full three dimensional CFD model.

2 Background

Swift [1] was the first to develop a theoretical framework of thermoacoustic devices based only on thermal interactions between the stack plates and the working fluid. In his quasi-one dimensional treatment, Swift ignored the fluid viscosity, and the plate's thermal conductivity in the stream-wise direction. He further assumed that the plates are much shorter than the acoustic wavelength and that the pressure oscillations are small compared to the mean pressure. The applicability of such idealized model is limited to linear system analysis. More recent workers showed substantial deviation of most cooling curves from Swift theory.

Different previous attempts [2-6] have been done in modeling thermoacoustic devices to predict the general performance, capture the thermal and viscous flow losses in the device, and help defining key variables affecting the design considerations and system optimization, such as stack porosity, size and location, working gas and appropriate operating mean pressure. Worlikar et al. [2,3] simplified the governing equations into a low-Mach number vorticity-based formulation. They were able to reduce the full computational domain into a single periodic thermoacoustic couple. Their model was however limited to short stack lengths, constant gas properties and small pressure amplitudes. Blanc-Benon *et al.* [6] further reported close agreement between the low-Mach-number simulation results and the particle image velocimetry (PIV) measurements of the flow field.

Worlikar approach was then traced in similar manners by Cao *et al.* [6], who constructed a first-order temporal and spatial discretization scheme to solve for the time-averaged energy flux density in the gas. Cao only considered short (compared with the particle displacement length) isothermal plates. Ishikawa and Mee [7] extended Cao's work to longer plates and investigated the effects of plate spacing using the PHOENICS finite-volume method, however, their single-precision calculations caused significant energy imbalances and restricted the overall accuracy in their heat fluxes results.

Latter, Marx and Blanc-Benon [8-11] constructed an explicit numerical model with symmetric boundary conditions which enables the prediction of the stack-heat exchangers coupling in TAR made of isothermal zero-thickness plates. They considered the time-averaged velocity field above the stack plate and observed the acoustic flow streaming above the plate. They further

identified the minimum plate length, compared to the particle displacement, enough for the generated temperature harmonics to get displayed above the whole plate surface. Although accurate, this model is too expensive computationally to limit its applicability to devices operating at high-frequency ranges (Their frequency value $f = 20$ kHz), which is useful for miniaturization purposes.

Zoontjens *et al.* [12] was the first to implement a FLUENT model to simulate the flow and energy fields in a TAR couple of non-zero thickness at a wide range of drive ratio ($1.7\% - 8.5\%$) and 200 Hz operating frequency. They assumed symmetric computational domain and investigated the time-averaged heat transfer through the stack material. Their model however used a first-order discretization scheme which in turn affected the accuracy of their numerical results. This was recently followed by the work of Tasnim and Fraser [13] who introduced a two-dimensional model using the STAR-CD finite volume solver. He assumed a periodic thermoacoustic couple and described the laminar-flow and thermal fields at low drive ratio 0.7%.

Other numerical simulations for thermoacoustic refrigerators have been reported [14,15]. However, none of them was able to predict the refrigerator general performance in the non-linear regime of acoustic excitations. To our knowledge, no efficient CFD simulation has been developed which models the large-amplitude excitations of standing TARs. Therefore, it is the goal of this work to develop a CFD model of TAR which helps understanding the flow properties in the non-linear regime and enables the prediction of the refrigerator performance and the secondary flow effects such as flow streaming and microstructural vortices.

3 Proposed Approach

3.1 Overview of Proposed Approach

We propose a CFD simulation for the oscillating flow behavior of large-scale half-wavelength standing thermoacoustic refrigerators. The developed computational model only considers the working ideal gas, the stack plates and resonator solid walls. For simplicity, our TAR is assumed to initially work at no load and hence the two heat exchangers are omitted in the current runs. The simulation allows the prediction of the bulk flow properties within the helium-gap and at the stack neighborhood, and focuses on the acoustically-driven steady-state temperature gradient across the stack plates. It also enables us to explore the mutual thermal and viscous interactions between the stationary solid plates and the surrounding ideal gas, and examine the micro-structural vortices developed at high-amplitude acoustic excitations.

It is unreasonable to numerically model the entire domain of resonator at the macroscopic scale, which may contain large number of uniformly repeated stack plates and air flow channels confined within a small volume of the resonator. The stack plates are also much shorter than the acoustic wavelength. This creates an additional scale complexity. Instead, we concentrate on a representative unit cell within the main domain, and impose appropriate boundary conditions at the cell surfaces.

We choose a two-dimensional unit cell, with horizontal edge of length B times the stack length l and vertical edge of length corresponds to helium-gap distance h, as a computational domain. To ensure that the enclosed thermoacoustic couple closely behaves as a representative part of the entire refrigerator, periodic boundary conditions are enforced on the cell horizontal surfaces, while ideal and equivalent acoustic flow conditions are supplied at the cell vertical surfaces. This approach also allows us to reduce the resonator edge effects.

The unit cell is initially filled with helium with ideal gas approximation at nearly ambient conditions. To generate the thermoacoustic effect, the cell is then subjected to low and high acoustic excitations through its transversal edges. This causes small- and large-amplitude oscillations to be introduced into the system, respectively. Simulations are performed using the non-linear CFD solver in ANSYS FLUENT. The first advantage of using ANSYS FLUENT is that it allows us to model the system response at either low or high drive ratios through its non-linear package. The second advantage is that the conjugate heat transfer algorithm enables us to account for the thermal interactions between the stack walls and the confined gas, and set the model parameters to accurately capture the temperature gradient across the stack plates.

Both refrigerator solid and gas domains are modeled by a series of 2D quadrilateral and triangular computational elements. The number and size of quadrilateral elements can be altered to provide accurate results at convenient computational cost. The simulation predicts the system steady-state response of the combined structure in terms of the stack walls static temperature and characterizes the periodic flow microstructures. The rest of this section presents the numerical representation of the TAR geometry including the stack size and location, and describe the domain meshing used in the simulation. The following section explains the application of the periodic and oscillating boundary conditions. Details of the numerical analysis using ANSYS FLUENT solver capabilities, such as controlling the time incrementation to maintain stable and fast-converging calculations are then presented. We finally discuss the simulation results in comparison with experiment and previous numerical attempts.

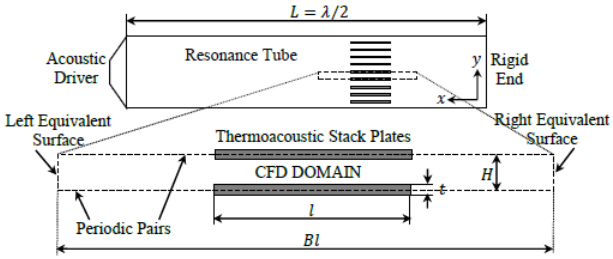

Figure 1: Schematic of the thermoacoustic refrigerator is shown on top. Bottom: The representative simulation unit cell has two periodic surfaces and two surfaces with equivalent boundary conditions.

Table 1: TAR Geometry Details and Stack Material Properties

l, mm	t, mm	H, mm	L, mm	ρ^s_{eff}, Kg/m^3	$C^s_{p,eff}$, J/kg K	k^s_{eff}, W/m K
6.85	0.19	1.53	1220	5082	683.5	5.76

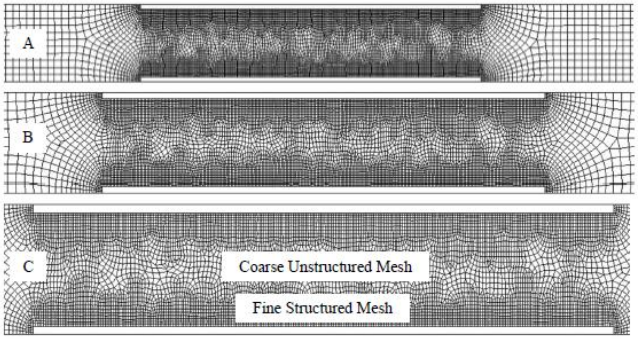

Figure 2: Three front cross-sectional views of the stack plates and the comprised helium. The Subplot A shows the computational cell domain. Subplots B and C show close-up views of the fine structured mesh at the stack surface and around its edges. Plate meshing is not shown.

3.2 Geometry and Domain Meshing

Figure 1 shows the geometry of the half-wavelength thermoacoustic refrigerator being modeled and tested, as described by Atchley *et al.* [4]. The resonator tube is made of copper and has a length L of 1.22 m. It has the acoustic driver at one end and closed at the other end. The resonator is filled with Helium at nearly ambient conditions. The stack plates are 6.85 mm long and composed of fiber-glass laminates of thickness 0.1016 mm each epoxied to 0.0889-mm-thick stainless steel plates. In our calculation, the stack location is variable and the spacing h between the plates is 1.338 mm. The TAR geometry details and the combined stack material properties, including the effective density ρ_{eff}^{s}, specific heat at constant pressure $C_{p,eff}^{s}$ and thermal conductivity k_{eff}^{s}, are indicated in Table 1.

The simulation unit cell is also plotted in Figure 1. The plot illustrates the geometry and boundary conditions of the comprised two-dimensional CFD domain. The cell has two horizontal surfaces with periodic boundary conditions (or, simply referred to as "periodic pairs") and two vertical surfaces with acoustic flow conditions that correspond to the idealized standing wave predictions at these locations. Although this approximation does not allow for accurate replication of the physical process at these boundaries, it can still suggest appropriate modeling at the far-field of the stack plates provided that the distance from the two vertical surfaces to the stack ends are big enough. For comparison, the simulation cell length and height are chosen to match values used by Worlikar simulation. Also, the constant B is 4.64 in the current simulation.

The stack domain is discretized into 2192 quadrilateral elements, while the gas domain is divided into 9621 mixed elements. The microstructural analysis indicates high smoothing and slow transition meshing at proximities and curvatures. The smallest element is 25 μm in size and the minimum number of elements across the gap is ten. A very fine structured mesh is thus enforced very close to the stack plates to accurately capture the thermoacoustic effect within the developed thermal penetration, while a coarser unstructured mesh is generated farther where the thermal interactions with the working gas are expected to vanish. For instance, the mesh of Figure 2 consists of 11758 elements and 12227 nodes. In our analysis, the thermal and viscous penetration depths, defined in terms of the gas thermal conductivity k^f and the gas dynamic viscosity μ respectively, are such that $\delta_k = \sqrt{2k^f/\rho_m\, C_p\omega} = h/4.97$ and $\delta_v = \sqrt{2\mu/\rho_m\omega} = h/6.02$, and the smallest mesh size is equal to $\delta_k/10.80$.

3.3 Boundary Conditions

To create a compact periodic structure, conformal periodic pairs are assigned to the computational solid and gas nodes lying on the horizontal surfaces of the simulation cell. This allows an equal air flow, to that leaving the simulation unit cell at one surface, to get introduced at its corresponding image surface. Similarly, the heat flux, rejected at one surface, is fully gained at its opposite periodic surface. In the current numerical model, both left and right equivalent surfaces are replaced by moving rigid walls. A layering dynamic mesh is allowed at the left and right vertical walls of the computational domain. The split and collapse factors are both set equal to 0.4, and a cell height of 0.13895 mm is used. A pre-processing program is developed to define the horizontal motions of the vertical walls' centers of gravity following the local ideal standing wave propagation,

$$u_{wall} = u_a \sin(kx)\cos(\omega t) \tag{1}$$

Here, u_a represents the oscillating boundaries' velocity amplitude, k is the wave number, x refers to the location of the equivalent surfaces, measured from the rigid end, and ω is the angular velocity. Further, u_a is expressed in terms of the acoustic pressure amplitude p_a, the mean density ρ_m and the speed of sound a as,

$$u_a = p_a/\rho_m a \tag{2}$$

The amplitude of the acoustic pressure p_a is the gas mean-pressure times the acoustic drive ratio. According to Atchley experimental study, the helium mean pressure p_m and temperature T_m are 114.1 kPa and 298.4 K respectively, and the frequency is 696 Hz. In our calculation, heat is not allowed to flow across the equivalent surfaces and the no-slip shear condition is satisfied. The stack inner walls are kept stationary with the no-slip shear condition used to describe the viscous interaction with the surrounding fluid. At the solid/fluid interfaces, thermally coupled boundary conditions are imposed to simulate the thermal interactions between the solid stack walls and the surrounding air particles through the conjugate heat transfer algorithm. In such case, ANSYS FLUENT requires that the temperature and the heat transfer to the wall boundary from a solid element match the fluid side heat transfer,

$$T_t^f = T_t^s \tag{3}$$

$$k^f \frac{\partial T^f}{\partial n} = k_{eff}^{s} \frac{\partial T^s}{\partial n} \tag{4}$$

where n is the local coordinate normal to the wall, and k^f is the fluid thermal conductivity.

3.4 ANSYS FLUENT Analysis

TRL[1]'s DELL Precision WorkStation (Intel® Xeon® X5690) is used to perform our simulations. ANSYS FLUENT is computationally efficient for the non-linear flow analysis with complicated oscillating and periodic boundary conditions. It solves the governing equations using a pressure-based finite volume method [16]. Its first-order implicit time algorithm usually requires many small time increments that allow the solution to proceed with fewer numbers of iterations per time increment. Double-precision parallel computation is essential to this analysis, therefore, the domain is divided into four partitions using the bisection method (Principal Axes), and the simulation uses four local parallel processors, maximum CPU hours of 50 and corresponding memory usage of two Gigabytes. The default bisection method (principal axes) and the smooth optimization method are used for mesh partitioning.

One crucial key in using ANSYS FLUENT is the time increment size. This is of extreme importance for two reasons: first to maintain a convergent simulation with minimal number of iterations –thus, minimizing the computational cost– and second to accurately capture the thermoacoustic cycling process. This justifies the use of a fixed time increment Δt of one hundredth of the applied excitation load period τ. The total real-flow time to reach the quasi-steady-state is almost five seconds and the simulation takes approximately 3×10^5 time increments for the system to reach its thermal equilibrium (or, energy balance).

In our double-precision calculations, convergence is claimed when the absolute variation in each of the flow quantities (residuals) is less than $10^{-4}\%$ (convergence criteria) in any two successive iterations. The maximum allowed number of iterations is 100 in each time increment, however approximately twenty iterations are sufficient to reach convergence because of our prior choice of small-size time increment. The 2nd order upwind spatial discretization scheme is used and the high-accuracy pressure staggering scheme (PRESTO) is enabled as the pressure interpolation scheme at the computational element faces. This scheme uses the discrete continuity balance for a staggered control volume about a face to compute the face corresponding pressure. PRESTO is recommended for flows involving porous media and high swirling flows when the pressure profile has a high gradient at the elements' faces. The pressure-implicit with splitting of operators (PISO) pressure-velocity coupling scheme is applied. The realizable k-ε turbulence model and the standard wall functions, suggested by Launder and Spalding [17], are used in the current CFD analysis. The calculation results however predicts a very low Reynolds number prevails with a fairly subcritical (laminar) separated vortical flow at the stack ends.

4 Data Post-processing

ANSYS FLUENT does not provide a direct way to calculate how much acoustic power is converted each time increment through the thermoacoustic stack into refrigeration effect. It only reports the acoustic pressure and velocity at each node. To learn more about the refrigerator coefficient of performance (COP), a post-processing program was written to use the values of the local acoustic pressure and *x*-velocity and calculate their product at each point of the flow field. The simplest way to calculate the time-averaged acoustic power is by summing the above product at every time increment and dividing by the number of time increments in one cycle N. In practice, in order to reduce the computational cost and focus on the quasi steady-state response, only the last acoustic cycle (with $N = 100$) is considered for the averaging process. The amount of the converted acoustic power is further estimated, according to Swift and Nijeholt *et al.* [1, 18]:

$$\dot{W} = \overline{p\,u} = \frac{1}{N}\sum_i p_i u_i \tag{5}$$

$$\bar{P} = \int_{hot} \overline{p\,u}\; dA - \int_{cold} \overline{p\,u}\; dA \tag{6}$$

For the sake of comparison with previous theoretical studies, the following equation defines the theoretical temperature difference, according to Wheatley *et al.* [19], as function of geometrical parameters, the thermal penetration depth δ_k, the viscous penetration depth δ_v, the gas constant γ and the Prandtl number $\sigma = C_p\mu/k^f$:

$$\Delta T = \frac{\dfrac{p_a^2\delta_k\left(1+\sqrt{\sigma}\right)\sin 2kx}{4\,\rho_m c[(k_{eff}^s t + k^f h)/l](1+\sigma)}}{1+\dfrac{p_a^2\delta_k\left(1-\sigma\sqrt{\sigma}\right)(1-\cos 2kx)}{4\,\rho_m T_m l\,\omega\left[(k_{eff}^s t + k^f h)/l\right](\gamma-1)(1-\sigma^2)}} \tag{7}$$

5 Results to date and Discussion

Four simulation runs are carried out at drive ratios 0.28%, 0.5%, 1.0% and 2.0%. In this work, the stack position is maintained fixed such that the corresponding non-dimensional wave number $kx = 3\pi/4$, measured from the resonator rigid end to the stack's middle section ($k = 2\pi/\lambda$). The thermoacoustic energy conversion is theoretically expected to peak at such stack location. Initially (at a simulation time $t = 0$), the helium-filled TAR system has a uniform temperature distribution of 298.4 K and zero gas velocity. The system is perturbed at its left and right equivalent boundaries through the oscillatory motions that carefully match the propagation of an ideal standing wave. Each of the four runs is then allowed enough time until the temperature difference ΔT across the stack approaches its quasi-steady state. We observe that five seconds are sufficient to achieve such limit within a reasonable CPU time of about 50 hours.

In practical thermoacoustic refrigerators, thermal energy is initially transported along the x-direction by the hydrodynamic transport of entropy carried by the velocity oscillations of the working gas [1]. The present non-isothermal stack plates allow for a temperature gradient to develop as the simulation proceeds, as shown in Figure 3(a), due to thermoacoustic heat-pumping effect. This causes the temperatures of the stack hot and cold ends to reach their upper and lower limits respectively then to further increase nearly at the same rate by viscous heating while closely maintaining a constant temperature difference across the stack. This then leads to an increase in the mean temperature of the stack plates.

[1] American University in Cairo's Thermoacoustic Research Lab

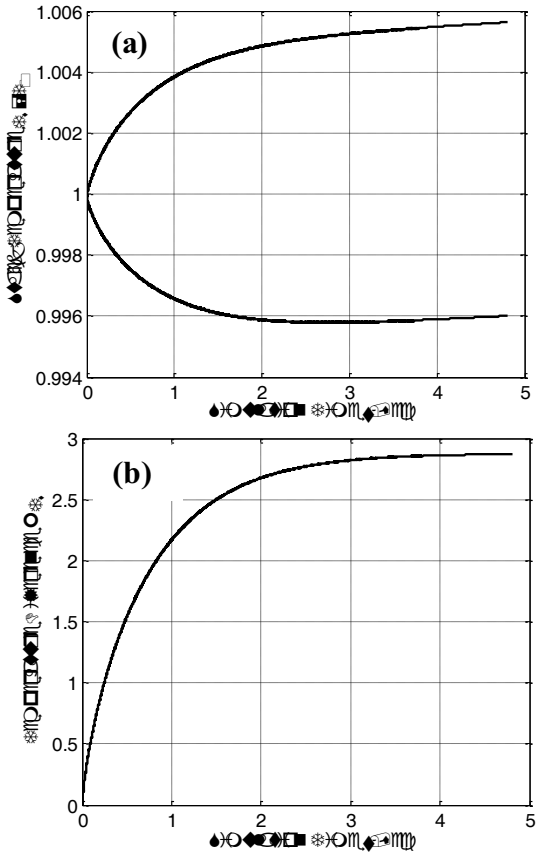

Figure 3: (a) Time-history of the hot and cold stack ends area-weighted temperatures for a drive ratio of 2%. The stack is placed at $kx = 3\pi/4$, where the thermoacoustic energy conversion is expected to peak. (b): Stack temperature difference showing convergence.

Figure 3(b) demonstrates convergence in the stack ends temperature difference as the computation proceeds. To understand this behavior, the numerical time-averaged temperature distribution along the stack plates, over the last acoustic period, is calculated and plotted in Figure 4 with comparison to the corresponding linear distribution at 2% drive ratio.

The theory assumed a linearly constant temperature distribution along the plates and ignored both fluid and solid thermal conductivities in the *x*-direction as well as the viscous dissipation, which in turn causes the ideal behavior in figure. However, a smoother slope than that predicted by theory, along with slight curvatures near the plates' ends is found in the current simulation. This is possibly because the stack plates' thermal conductivity allows for the heat flow due to conduction down the stack temperature gradient (heat loss), in addition to the heat transferred by the net mass flux resulted from the acoustic streaming. This causes the temperatures of the stack hot and cold ends to further smooth out to their indicated quasi-steady state values.

Therefore, a close agreement is noticed between the slopes of the current distribution and the corresponding theoretical trend close to the middle section of the stack plates while a strong deviation is captured around the stack ends. This effect is expected to become of lesser importance than that of viscous heating at high drive ratios, especially when using shorter stack plates with smaller thermal conductivities. To investigate the effect of nonlinearities associated with high-amplitude excitations on the generated temperature gradient, Figure 4 compares the temperature difference ΔT across the stack as a function of

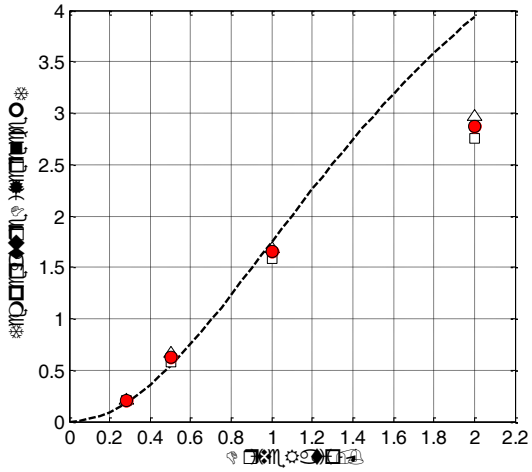

Figure 4: The change in the stack ends temperature difference as function of the drive ratio. The stack is placed at $kx = 3\pi/4$. The dashed line refers to the theoretical temperature difference, as derived by Wheatley *et al.* [19] in Eq. 7. Symbols: Open triangles and squares are the Atchley experimental values and the Worlikar numerical results, respectively, while the red closed circles represent the current simulation.

the acoustic drive ratio to Atchley's experimental values, Wheatley's linear theory for thermoacoustic devices and Worlikar numerical results. Interestingly, the current numerical methods replicate the non-linear behavior captured in the quasi-steady experimental measurements. The system behavior is clearly nonlinear at drive ratios greater than 1% because of the high-amplitude pressure excitations. As a result, the nonlinear propagation of high-amplitude excitations promotes the generation of harmonic oscillations and the acoustic flow streaming within the stack and surrounding the stack ends.

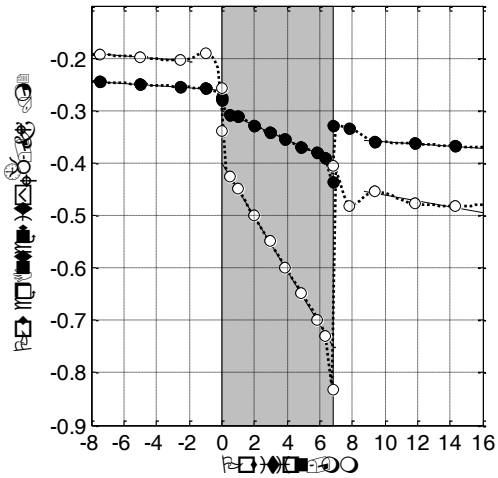

Figure 5: Longitudinal variation of the area-weighted time-averaged of the power intensity at drive ratio **2**%. Closed and open symbols refer to thin and thick plates respectively. The gray area points out the stack region. The dotted lines are shape-preserving interpolant for both dataset. Solid lines are three separate linear fits for the pre-stack resonator, stack and post-stack resonator regions.

5.1 Acoustic Power

As discussed in the data post-processing section, the intensity of the acoustic power is calculated and recorded during the last acoustic cycle, in which hundred time steps are used for computation. A special program is developed

to evaluate the time-averaged component of the acoustic power. In Figure 5, the behavior of the acoustic power is distinguished into three regions; with the stack left end is closer to the driver side. First, the pre-stack and post-stack resonator sections are characterized by almost similar decreases in the power intensity because of the acoustic thermal loss. The stack section however exhibits higher degradation in the acoustic power with larger slope. This is mainly due to the acoustic energy conversion into heat pumping between the stack ends, in addition to the accompanying thermal and viscous losses which result from the interactions of the gas particles with the stack plates.

The simulation reveals significant sudden drop in the acoustic power at the left stack end while a corresponding abrupt jump is observed at the right stack end which extends few millimeters into the post-stack resonator. This reflects the secondary flow losses associated with the sudden contraction and expansion of the oscillating-flow at the edges of the stack plates which are caused by the immediate change in the viscous boundary conditions at these locations. Such geometrical constraints also provoke the separation of the boundary layers and induce the formation of the vortical motions beyond the stack region.

The current CFD model is further applied to a modified TAR system with thicker stack plates to study the effect of plate thickness -thus, the stack porosity- on the consumed acoustic power and evolving microstructure on top of the plates' surfaces and near the stack ends. The plate thickness has increased such that the spacing between the stack plates becomes three times the thermal penetration depth and four times the viscous penetration depth.

6 Conclusion

ANSYS FLUENT is a useful tool that allows us to directly simulate the gas dynamics of non-linear oscillating compressible-flow of half-wavelength thermoacoustic refrigerators, and enables the detection of thermoacoustic cooling effect between the stack ends and the prediction of the consumed acoustic power during the acoustic loading through its computational fluid dynamics solver and the conjugate heat transfer algorithm. The simulation results agree well with Atchley experimental values and capture the general behavior of the thermo-acoustically-induced vortical motions at the stack ends and flow streaming, provided that the condition of no slipping at the stack plates' surfaces is satisfied.

Acknowledgment

The work presented here is supported by the King Abdullah University for Science and Technology (KAUST).

References

[1] G. W. Swift, "Thermoacoustic Engines", *J. Acoust. Soc. Am.*, 84-4, 1145-1180 (1988)

[2] A. S. Worlikar, O. M. Knio, "Numerical Simulation of a Thermoacoustic Refrigerator. I. Unsteady Adiabatic Flow", *J. Comput. Phys.*, 127, 424-451 (1996)

[3] A. S. Worlikar, O. M. Knio, R. Klein, "Numerical Simulation of a Thermoacoustic Refrigerator. II. Stratified Flow around the Stack", *J. Comput. Phys.*, 144, 299-324 (1998)

[4] A. A. Atchley, T. J. Hofler, M. L. Muzzerall, M. D. Kite, C. Ao, "Acoustically Generated Temperature Gradients in Short Plates", *J. Acoust. Soc. Am.*, 88-1, 251-263 (1990)

[5] R. L. Panton, "*Incompressible Flow*", John Wiley & Sons, Inc. (1996)

[6] N. Cao, J. R. Olson, G. W. Swift, S. Chen, "Energy Flux Density in a Thermoacoustic Couple", *J. Acoust. Soc. Am.*, 99-6, 3456-3464 (1996)

[7] H. Ishikawa, D. J. Mee, "Numerical Investiations of Flow and Energy Fields near a Thermoacoustic Couple", *J. Acoust. Soc. Am.*, 111- 2, 831-839 (2002)

[8] P. Blanc-Benon, E. Besnoin, O. Knio, "Experimental and Computational Visualization of the Flow Field in a Thermoacoustic Stack", *CR Mechanique*, 17-24 (2003)

[9] D. Marx, P. Blanc-Benon, "Numerical Simulation of Stack-Heat Exchangers Coupling in a Thermoacoustic Refrigerator", *AIAA J.,* 42-7, 1338-1347 (2004)

[10] D. Marx, P. Blanc-Benon, "Computation of the Mean Velocity Field above a Stack Plate in a Thermoacoustic Refrigerator", *CR Mechanique*, 332, 867-874 (2004)

[11] D. Marx, P. Blanc-Benon, "Computation of the Temperature Distortion in the Stack of a Standing-Wave Thermoacoustic Refrigerator", *J. Acoust. Soc. Am.*, 118-*5*, 2993-2999 (2005)

[12] L. Zoontjens, C. Q. Howard, A. C. Zander, B. S. Cazzolato, "Numerical Study of Flow and Energy Fields in Thermoacoustic Couples of Non-Zero Thickness", *Int. J. Therm. Sci*., 48, 733-746 (2009)

[13] S. H. Tasnim; R. A. Fraser, "Computation of the Flow and Thermal Fields in a Thermoacoustic Refrigerator", *Int. Commun. Heat Mass*., 37-7, 748-755 (2010)

[14] F. Zink, J. S. Vipperman, L. A. Schaefer, "Advanced Thermoacoustics through CFD Simulation Using FLUENT", *Proc. IMECE 2008*, 101-110 (2008)

[15] A. Piccolo, G. Pistone, "Numerical Study of the Performance of Thermally Isolated Thermoacoustic-Stacks in the Linear Regime", *Proc. Acoustics 2008*, 3555-3560 (2008)

[16] H. K. Versteeg, W. Malalasekera, "*An Introduction to Computational Fluid Dynamics. The Finite Volume Method*", Longman Group Ltd., England (1995)

[17] B. E. Launder, D. B. Spalding, *"The Numerical Computation of Turbulent Flows", Comput. Methods Appl. Mech. Eng*., 3, 269-289 (1974)

[18] J. A. L. Nijeholt, M. E. H. Tijani, S. Spoelstra, "Simulation of a Traveling-Wave Thermoacoustic Engine Using Computational Fluid Dynamics", *J. Acoust. Soc. Am*., 118-4, 2265-2270 (2005)

[19] J. Wheatley, T. Hofler, G. W. Swift, A. Migliori, "An Intrinsically Irreversible Thermoacoustic Heat Engine", *J. Acoust. Soc. Am.*, 74, 153–170 (1983)